U.P.B. Sci. Bull., Series D, Vol. 76, Iss. 2, 2014 ISSN 1454-2358

PARAMETER STUDY OF ACTIVE FLOW CONTROL ON A HIGH LIFT AIRFOIL

Andreea BOBONEA[1], Corneliu BERBENTE[2], Mihai Leonida NICULESCU[3]

Active manipulation of separated flows over airfoils at high angles of attack has been the focus of a number of investigations of many scientists and engineers in fluid mechanics. The objective of these investigations is to improve the aircraft aerodynamic performance by delaying the boundary layer separation. One of the main methods used in active flow control is the usage of blowing devices with constant and pulsed blowing. Through unsteady CFD simulation over an airfoil, this study highlights the impact of slot width, blowing momentum coefficient and jet velocity, in enhancing the aerodynamic characteristics of an airfoil.

Keywords: Pulsed Blowing, Active Flow Control, Blowing Momentum, Jet Velocity, CFD, Unsteady, High-Lift Configuration

1. Introduction

Active manipulation of separated flows over airfoils at high angles of attack has been the focus of a number of investigations for many years. The objective of these investigations is to improve the aerodynamic performance and extend the flight envelope by delaying boundary layer separation. The prevention of separation and the generation of high lift without changing angle of attack or flap deflection are beneficial in many areas (an important aspect of flow control) [1].

Active flow control investigations for separation control on an airfoil have employed a variety of techniques including external and internal acoustic excitation, vibrating mechanical flaps, and steady and unsteady blowing. Research in this area is blooming and the potential performance benefits are very encouraging [2, 3, 4]. Previous numerical investigations focused on obtaining the best performance of AFC with regard of dynamic parameters, blowing momentum coefficient C_μ, actuation frequency F^+, and actuation orientation [5, 6].

[1] Ph. D. Student, Aerospace Engineering Faculty, University POLITEHNICA of Bucharest, Romania, e-mail: andreea_911@yahoo.com
[2] Professor, Aerospace Engineering Faculty, University POLITEHNICA of Bucharest, Romania, e-mail: berbente@yahoo.com
[3] Scientific Researcher, National Institute for Aerospace Research "Elie Carafoli" - INCAS, Bucharest, Romania, e-mail: mniculescu@incas.ro

In addition to the previous studies, the present paper is focused on studying the impact of the velocity ratio (VR) and the blowing momentum coefficient (C_μ) and looking for the most trivial flow control parameter between the blowing momentum and the velocity ratio. The VR and C_μ could be studied decoupled by varying the slot width and the jet exit velocity where the other inflow and actuation conditions are constant. Such a variation of slot width was not available in the literature for the pulsed blowing through slots.

2. Computation Setup

The present studies have been performed on a high-lift airfoil (main airfoil and trailing edge flap) for transport aircraft. The airfoil coordinates were made available by DLR Braunschweig. Further details concerning the airfoil geometry can be found in Wild [7].

The flight conditions for this airfoil are infinite upstream Mach number M=0.15, the Reynolds number $Re=2\text{x}10^6$. In order to illustrate the capabilities of the pulsed blowing as active separation control technique a high lift configuration with flap deflection $\delta_F=49^0$, gap g_F/c=0.9%, overlap ovl_F/c=2.3% was investigated.

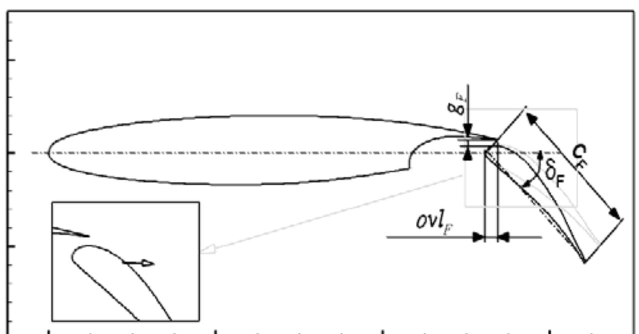

Fig. 1: Airfoil Configuration, $\delta_F=49^0$ (Source: Ciobaca [6])

The geometrical setup of the actuation was defined starting from a reference slot - actuator with a width of 0.3mm, located at 20% c_F on the flap section side, inclined 45^0 trigonometrically and the slot width was varied in {0.1; 0.15; 0.3; 0.45; 0.6; 0.9}mm.

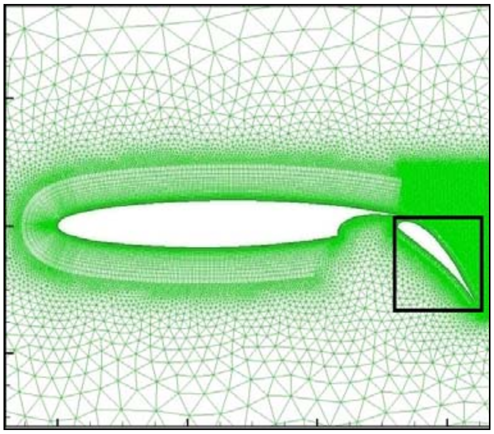

Fig. 2: Airfoil Mesh Configuration

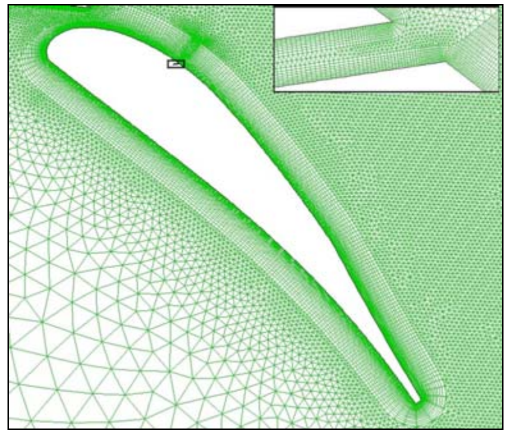

Fig. 3: Flap and Slot Meshing detail

The accuracy of the results obtained with CFD is highly depending on the density and quality of the computational grids. In the present study, hybrid grids were created using the commercial grid generation software Centaur (Fig. 2 and Fig. 3) [8]. The farfield boundaries are placed approximately 50 times the chord length (c=0.6m) upstream and downstream top and bottom from the airfoil leading edge.

To properly capture the boundary layer ($y^+\approx1$), the first layer thickness was calculated as being ds=7.4e-06m and the turbulent boundary layer thickness has a value of about 1.22cm. With the help of these values, the proper Number of quadrilateral layers (49 layers) and the stretching factor (1.1) were defined.

All the computations presented in this study were performed using the DLR–TAU Code [9]. The input parameters were defined as follows: Mach number of M=0.15, Reynolds number $Re=2*10^6$, static temperature T=293.15K and a static pressure of p=101325Pa. All simulations are carried out with an unsteady compressible Navier-Stokes solver. The one-equation model of Spalart and Allamaras [10] was used for turbulence modeling. The profile angle of attack is set to 0^0.

All unsteady simulations with time-varying jets were conducted using a dual time-step approach. For the numerical setting the actuation frequency f=100Hz guided the length of the dual time step, where Δt=1e-04s, with 500 inner iterations per time step and 10000 physical time steps. At very small slot widths, for reaching the targeted convergence, an increase at 750 inner iterations per time step was required. Because the present study is time accurate, it yields time history of the entire flow field, and thus the parameters of interest such as lift, drag and momentum coefficients as functions of time. For simplicity reasons, time averaged quantities; averaged over 100 physical time steps are presented and discussed.

The first simulation represents an analysis of a reference configuration without flow control. All later tests were performed with the actuation defined as pulsed-blowing actuation, with a standard incompressible jet.

For the standard incompressible jet boundary condition, the jet density ρ_{jet}, the jet velocity u_{jet} and the jet direction vector are imposed [11].

Usually the static pressure p_n is extrapolated from the first inner field point. Alternatively, the static pressure can be imposed, which in some cases increases stability and the speed up rate of the solution for this incompressible version of the actuation boundary condition. In case of unsteady blowing, $\rho|_{inlet}$ is kept constant in time and $u_{jet}(t)$ is varied. For pulsed blowing:

$$u_{jet}(t)= u_{jet,max}\,\varphi(t) \tag{1}$$

where φ(t) represents the smoothing of the top - hat signal.

The actuation was defined using the following parameters:

- Jet area [A_{jet}] = slot width [w]
- Actuation type = pulsed_blowing (constant_blowing, as reference)
- Actuation period = 0.01
- Actuation duty cycle =0.5
- Maximum jet velocity = dependent on the type of actuation used

For constant blowing simulation (used as reference), the maximum jet velocity describes the constant jet velocity and was set as $U_{jet,\ max}$=150m/s. For pulsed blowing. U_{jet} was extracted from the following formula:

$$C_\mu = \frac{\rho_{jet}\cdot U_{jet}^2 \cdot A_{jet}}{\rho_\infty \cdot U_{ref}^2 \cdot A_{ref}} \tag{2}$$

where slot width, *w*[mm] and blowing momentum coefficient, C_μ [%] are set using the values from the following table, U_{ref}=51.48m/s, A_{ref}=chord length=0.6m (2D study).

Table 1

Jet velocities as calculated with the previous formula

Slot Width [mm] / C_μ [%]	0.1	0.2	0.3	0.4	0.5
0.1	178.33	252.19	308.88		
0.15	145.6	205.92	252.19	291.21	325.58
0.3	102.96	145.60	178.33	205.92	230.22
0.45	84.06	118.88	145.6	168.13	187.97
0.6	72.8	102.96	126.09	145.60	162.79
0.9	59.44	84.06	102.96	118.88	132.92

3. Results

One of the most important parameters in describing an actuation, in our case pulsed-blowing actuation (with a squared-shape signal) is the blowing momentum coefficient. In Fig.4, we can see that by increasing the blowing momentum coefficient from 0.1 - 0.5%, the aerodynamic coefficients significantly change: the lift coefficient increases rapidly from 0.1% to 0.4%, afterwards the increase is slower; the drag coefficient decreases rapidly from 0.1% to 0.4%, afterwards the decrease is smaller.

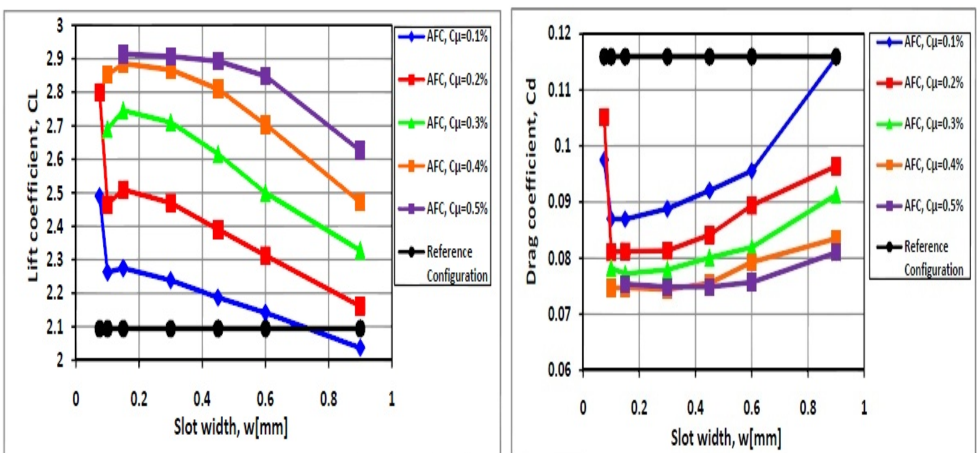

Fig. 4.: Lift and drag coefficient curves for $\alpha=0^0$ at M=0.15, $Re=2*10^6$, f=100Hz

Fig. 4 highlights also the importance of the slot width, so that the wider it is, the more efficient is the variation of the blowing momentum coefficient. Looking closely at the previous plots, it can be observed a small decrease of the lift coefficient from slot 0.15mm to 0.1mm.

The second parameter studied in this project is the jet velocity and his influence on the aerodynamic coefficients. In Fig. 5, it is presented a comparison for lift coefficients. It can be seen that the effectiveness of the blowing is increased, by increasing the velocity of the jet. As important as the jet velocity is the variation of slot width, highlighted in these plots by unifying constant velocities with black lines.

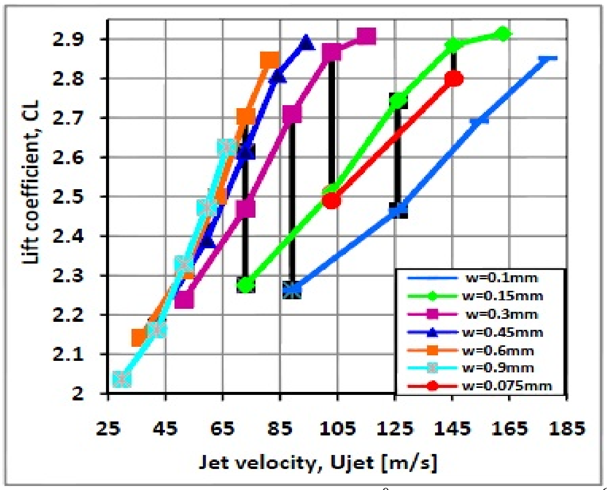

Fig.5.: Lift coefficients curves for $\alpha=0^0$ at M=0.15, $Re=2*10^6$

The pictures displayed in Fig. 6 and Fig. 7 show the corresponding numerical result of the surface streamlines on the main airfoil. On the upper surface of the flap, flow separation becomes visible by the direction of surface streamlines (see Fig. 6). The upwash - effect reduces the velocity near the wall of the main trailing edge. Thereby the flow above the trailing edge is subject to separation. By inducing high velocity jet on flap near the leading edge, before the separation occurs, the boundary layer separation is delayed.

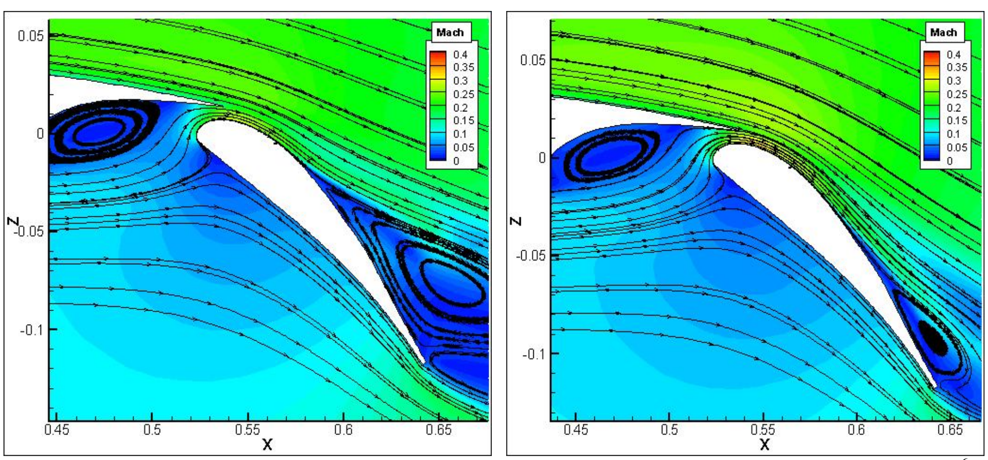

Fig.6. Mean flow streamlines and Mach number distributions for $\alpha=0^o$ at $U_\infty\approx$50m/s, $Re\approx2\text{x}10^6$; with AFC, f=100Hz, w=0.3mm, (C_μ=0.1% -left, C_μ=0.3% -right)

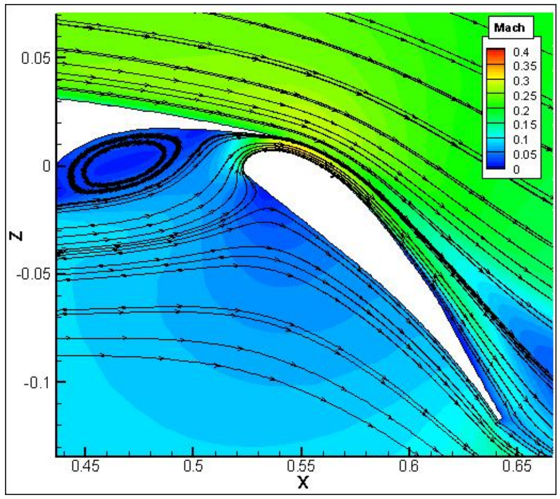

Fig.7. Mean flow streamlines and Mach number distribution for $\alpha=0^o$ at $U_\infty\approx50$m/s, $Re\approx2\text{x}10^6$; with AFC, f=100Hz, w=0.3mm, (C_μ=0.5%)

6. Conclusions

In the present study, a number of URANS simulations were performed on a 2D high-lift configuration, for investigation of active flow separation control with the use of pulsed blowing actuation. In addition to previous papers [5, 6] it was clearly showed the importance of the slot width, blowing momentum and jet velocity on the effectiveness of pulsed-blowing jet on a high-lift configuration. It was shown that for a constant mass flow, a narrower actuator is more efficient than a larger one. The second parameter studied in this paper is the jet velocity and his influence on the aerodynamic coefficients and one can see that the effectiveness of the blowing is increased, by increasing the velocity of the jet. For momentum blowing coefficient C_μ, in the range of 0.1% - 0.4% the effectiveness of pulsed blowing actuation is higher, as from 0.4% to 0.5% the changes are smaller. Up to now, all simulations were done for a single frequency, and it is known that the variation of this parameter is important in achieving the optimum performance for a configuration.

Acknowledgements

The work was performed within the EREA Mobility Programme, which has as primary objective getting in contact with different research groups, working with new tools, with new research fields like AFC.

The numerical investigations have been addressed during my stay at DLR Institute for Aerodynamics and Flow technology in Braunschweig, under the close supervision of Vlad Ciobaca and Ralf Rudnik.

The support of “University Politehnica of Bucharest” through the project “Burse doctorale: investitii in cercetare – inovare - dezvoltare pentru viitor (DocInvest) POSDRU/107/1.5/S/76813” is gratefully acknowledged.

R E F E R E N C E S

[1] *R. D. Joslin, D.N.Miller,* Fundamentals and Applications of Modern Flow Control, Published by American Institute of Aeronautics and Astronautics, ISBN 978-56347-983-0, 2008.

[2] *R. Petz* and *W. Nitsche*. Active Separation Control on the Flap of a Two-Dimensional Generic High-Lift Configuration. Journal of Aircraft, 44(3):865–874, 2007.

[3] *F. Haucke*, *I. Peltzer*, and *W. Nitsche*. Active Separation Control on a Slatless 2D High-Lift Wing Section. ICAS Paper 2008-175, 2008.

[4] *F. Haucke*, *M. Bauer*, *W. Nitsche*, and *B. Gölling*. An Active Flow Control Strategy for High-Lift Flaps. Proceeding of KATnet II Conference on Key Aerodynamic Technologies, Bremen, Germany, May 2009.

[5] *V.Ciobaca*, Parameter Study for a Slatless 2D High-Lift Airfoil with Active Separation Control using a URANS Approach, Notes on Numerical Fluid Mechanics and Multidisciplinary Design, Springer– Verlag, Vol. 121, Berlin, 2013, pp. 135-142.

[6] *V.Ciobaca,* Simulation of Active Flow Control on the Flap of a 2D High-Lift Configuration, Notes on Numerical Fluid Mechanics and Multidisciplinary Design, Vol. 112, Springer–Verlag, Berlin, 2010 pp. 209–216.

[7] *J. Wild*, Experimental investigations of Mach- and Reynolds-number dependencies of the stall behavior of 2-element and 3-element high-lift wing sections. AIAA Paper 2012-108, 2012.

[8] http://www.centaursoft.com

[9] T. *Gerhold* - Overview of the Hybrid RANS Code TAU. MEGAFLOW - Numerical Flow Simulation for Aircraft Design, Vol. 89 of Notes on Numerical Fluid Mechanics and Multidisciplinary Design, Springer, 2005, pp. 81-92.

[10] P. R. *Spalart*, S. R. *Allmaras,* A One-equation Turbulence Model for Aerodynamic Flows, Recherche Aerospatiale, No.1, 1994, pp 5-21.

[11] *T. Knopp,* The Actuation Boundary Condition for Flow Control in the DLR TAU Code, DLR Report, IB-Nr. 224 - 2010A44, DLR, Germany, 2010.